

## Modeling of the mechanism of hydrolysis of succinylcholine in the active site of native and modified (Asp70Gly) human butyrylcholinesterase

S. V. Lushchekina,<sup>a\*</sup> B. L. Grigorenko,<sup>b</sup> D. I. Morozov,<sup>b</sup> I. V. Polyakov,<sup>b</sup> A. V. Nemukhin,<sup>a,b</sup> and S. D. Varfolomeev<sup>a,b</sup>

<sup>a</sup>N. M. Emanuel Institute of Biochemical Physics, Russian Academy of Sciences,  
4 ul. Kosygina, 119334 Moscow, Russian Federation.

Fax: +7 (499) 137 4101. E-mail: sofia.lushchekina@gmail.com

<sup>b</sup>Department of Chemistry, M. V. Lomonosov Moscow State University,  
1 Leninskie Gory, 119992 Moscow, Russian Federation.

Fax: +7 (495) 939 0283. E-mail: anem@lcc.chem.msu.ru

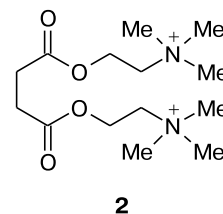
The quantum mechanics/molecular mechanics method was used to model the mechanism of hydrolysis of succinylcholine in the active site of native butyrylcholinesterase and the Asp70Gly single mutant enzyme. The energy diagram for the reaction pathway of the acylation was constructed, and the effect of the mutation on the reaction mechanism and energy characteristics of the process are discussed.

**Key words:** butyrylcholinesterase, succinylcholine, quantum mechanics/molecular mechanics method, reaction mechanism, effect of mutation.

Butyrylcholinesterase (BuChE, **1**), also called plasma cholinesterase or pseudocholinesterase, is widespread in various tissues, but is mainly present in the blood plasma and liver. The physiological function of this enzyme remains unclear. Nevertheless, it was reported that BuChE supposedly protects against poisoning with small doses of organophosphorus compounds<sup>1</sup> by binding part of toxic substances taken into the body, thus decreasing their acute toxicity. Butyrylcholinesterase is involved in the metabolism of a broad spectrum of endogenous and exogenous substrates and in the biotransformation of xenobiotics. In particular, the hydrolysis of cocaine by BuChE is the main metabolic pathway of elimination of this substance from the body.<sup>2</sup> Inactive precursors of many drugs are transformed into the active form during the metabolic activation through their hydrolysis by BuChE.<sup>3</sup>

Since BuChE-encoding genes are polymorphic, several enzymes with different levels of activity, including silent variant lacking the enzymatic activity, are formed in the body. The atypical isoform of BuChE is of most importance from the medical point of view. People with this genotype are characterized by the abnormal response to the introduction of the short-acting muscle relaxant succinylcholine (**2**), which is manifested in respiratory failure during 2–5 h.<sup>4</sup> Succinylcholine (or succinyldicholine) is an ester of two choline molecules joined to succinic acid bearing a double positive charge.

In 1989, it was already found<sup>5</sup> that a decrease in the activity of BuChE against **2** is associated with a single



mutation in the nucleotide 209 of GAT2GGT, which is reflected in the substitution of Gly for Asp70 in the protein. In this context, detailed investigation, including modeling and simulation, of the reaction mechanism of hydrolysis of **2** in the active site of BuChE and the effect of the Asp70Gly mutation on this mechanism is of great interest. However, the hydrolysis was poorly characterized in theoretical studies. For instance, only the second reaction step (deacylation) was considered.<sup>6</sup> In another study,<sup>7</sup> the hydrolysis of another substrate, viz., cocaine, was investigated.

Like in all serine hydrolases, the active site of BuChE is formed by the amino acid residues of the catalytic triad Ser198—His438—Glu325 (the numbering of amino acid residues in the present study is according to the crystallographic numbering for the structure PDB ID: 1P0P). It is located at the bottom of a 20 Å-long narrow gorge. The oxyanion hole formed by the peptide NH groups of Gly116, Gly117, and Ala199 is an important component of the active site. These residues hold the carbonyl oxygen atom of the substrate by hydrogen bonds. The amino acid resi-

dues Glu197, Trp82, and Tyr332 form the anionic site, and the mutation of any of these residues leads to a decrease in the rate of catalysis.<sup>8</sup> According to the commonly accepted mechanism of catalysis by serine proteases,<sup>9</sup> the hydrolysis occurs in two steps. The acylation step involves the nucleophilic attack of the oxygen atom of Ser198 on the carbonyl carbon atom of the substrate giving a tetrahedral intermediate followed by the release of the choline molecule. In the second step, the acyl-enzyme that is formed in the first step is subjected to deacylation.

Modern molecular modeling methods, such as molecular docking, molecular dynamics, quantum chemistry, and the quantum mechanics/molecular mechanics (QM/MM) approach, provide detailed information on the mechanisms of enzymatic reactions at the atomic level. Previously, this method has been used to study the hydrolysis of the hexapeptide fragment in the active site of sedolisin,<sup>10</sup> of guanosine triphosphate by the proteins RAS and RAS-GAP,<sup>11</sup> of adenosine triphosphate by myosin,<sup>12</sup> and of acetylcholine in the active site of acetylcholinesterase.<sup>13,14</sup> All these studies showed a good agreement between the results of calculations and the experimental structural and kinetic data.

The aim of the present study was to investigate the effect of the Asp70Gly mutation in butyrylcholinesterase on the energy profile of the hydrolysis of **2** for the acylation step by the QM/MM method.

### Models and Methods

The model system for the calculations was constructed based on the crystallographic structure from the Protein Data Base (PDB)<sup>15</sup> with the PDB ID 1P0P solved at 2.7 Å resolution. The peptide groups of the central fragment of a radius of approximately 20 Å about the catalytic triad were used. Geometry optimization was performed with the fixed positions of the atoms located at distances longer than 8–10 Å from the active site.

The hydrogen atoms, which are absent in the crystallographic structure, were added using the Reduce program.<sup>16</sup> The determination of the ionization state of His438 is of importance for the subsequent modeling of the hydrolysis. According to the commonly accepted mechanism<sup>17</sup> of hydrolysis of esters by cholinesterases, the first acylation step involves the nucleophilic attack accompanied by the proton transfer from the oxygen atom of Ser198 to the nitrogen atom of His438, whereas the transfer of the second proton from the nitrogen atom of histidine to Glu334 is still debated.<sup>18</sup> These two facts provide unambiguous evidence that in the enzyme–substrate complex, His438 exists in the uncharged state, the orientation of the imidazole ring being such that the proton is at the N<sup>δ</sup> atom of His438. In the crystallographic protein structure, the distance between the oxygen atom of Ser198 and the nitrogen atom of His438 is too large (3.27 Å) for the proton transfer to occur during the nucleophilic attack. This can lead to an artificial overestimation of the energy barriers. To preclude this situation, the orientation of the histidine residue was corrected, and the distance between the above-men-

tioned atoms was 2.7 Å. The subsequent geometry optimization of the enzyme–substrate complex by the QM/MM method showed that this correction was adequate. Thus, this distance was decreased to 2.5 Å, whereas this important result was not achieved for the initial conformation.

Molecule **2** was placed in the model structure using the molecular docking (Autodock 3.0 program).<sup>19</sup> The water molecules located in the cavities formed by the side chains of the amino acid residues in the vicinity of the active site play an important role in the reaction, but not all of them are present in the crystallographic structure. Therefore, cavities in the vicinity of the active site were searched for using the TINKER 3.7 program.<sup>20</sup> Cavities thus located were filled with water molecules whose positions, as well as the position and conformation of the substrate molecule, were then optimized by the molecular dynamics annealing. The molecular dynamics simulation was carried out using the TINKER program package and the MMFF94 force field<sup>21</sup> by varying the temperature from 0 to 300 K and in the reverse direction with a total duration of 200 ps.

The starting geometric configuration of the system (1950 atoms) thus obtained was used in the QM/MM calculations.

When constructing the model system for QM/MM calculations, it is very important to separate the quantum-mechanical and molecular-mechanical subsystems. The former subsystem should include molecules or amino acid residues, which are directly involved in chemical transformations and influence the electron density distribution in the system. The quantum-mechanical subsystem used for the simulation of the acylation step included molecule **2** and the side-chain atoms of the amino acid residues of the catalytic triad Ser198–His438–Glu325 directly involved in the catalysis (a total of 25 atoms, Fig. 1).

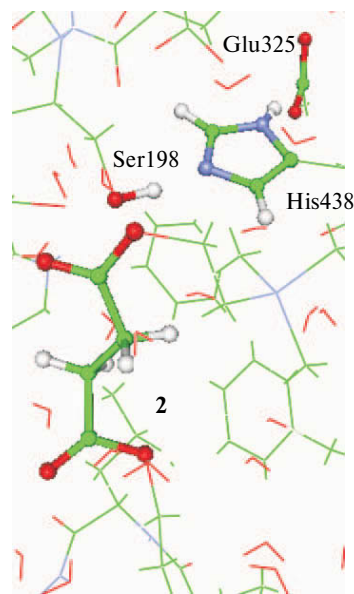


**Fig. 1.** Quantum-mechanical subsystem.

*Note.* Figs 2–5 are available in full color in the on-line version of the journal (<http://www.springerlink.com/issn/1573-9171/current>) and on the web-site of the journal (<http://russchembull.ru>).

All other atoms of the model system were assigned to the molecular-mechanical subsystem. The model for the modified enzyme was constructed by the substitution of Gly for the residue Asp70 in the starting structure.

The equilibrium geometric configurations were refined by the flexible effective fragment QM/MM method<sup>22,23</sup> using the parameters of the AMBER 99 force field,<sup>24</sup> which was implemented in the PC GAMESS 7.1.F program package,<sup>25</sup> to account for interactions between the fragments. The energies and forces in the quantum subsystem were calculated by the restricted Hartree–Fock method with the cc-pVDZ basis set.

The energy barriers for all regions of the acylation step were calculated using an appropriate interatomic distance taken as the reaction coordinate. Since the true reaction coordinate was unknown, several possible reaction coordinates were used to estimate the energy barriers to the acylation and deacylation steps. For example, simultaneous scanning along the  $R(\text{O}_{\text{Ser198}}-\text{C}_{\text{SuCh}})$  and  $R(\text{O}_{\text{Ser198}}-\text{H}_{\text{Ser198}})$  reaction coordinates was carried out for the acylation step. It appeared that in this case the reaction coordinate is a linear combination of the  $R(\text{O}_{\text{Ser198}}-\text{C}_{\text{SuCh}})$  and  $R(\text{O}_{\text{Ser198}}-\text{H}_{\text{Ser198}})$  coordinates. The intermediate geometric configurations of the system corresponding to the points on the potential energy surface (PES) between the local minima were obtained by varying the reaction coordinate from the initial to the final value with a specified increment ( $\sim 0.1$ – $0.2$  Å). The coordinates of the other atoms in the starting configuration were determined by the linear interpolation of the values for the geometric configurations corresponding to the stationary points on the PES. Each starting intermediate geometric configuration was optimized in the calculations at a fixed current value of the reaction coordinate.

## Results and Discussion

The calculations gave a set of stationary points on the PES of the model molecular system corresponding to the

reaction proceeding from the enzyme–substrate complex to the acyl-enzyme through the tetrahedral intermediate along the assumed reaction coordinates. We also calculated the energy barriers to the reaction steps for the native and modified enzymes.

The superimposition of the enzyme–substrate complexes for the modified and unmodified enzymes is shown in Fig. 2. It should be noted that the geometric configurations of the residues of the catalytic triad remain virtually unchanged. The introduction of the mutation leads to a slight shift of the substrate (because the charged amino acid is replaced by the uncharged amino acid) and, consequently, to a decrease in the binding energy.

The enzyme–substrate complex (Fig. 3) corresponds to the geometric configuration of the reactants in the beginning of the reaction. The planarity of the ester group of succinylcholine ( $\text{RC}-\text{C}(\text{O})-\text{OCH}_2\text{R}$ ,  $\sim 170^\circ$ ) is indicative of the  $\text{sp}^2$  hybridization of the carbonyl carbon atom of the substrate. The  $R(\text{H}_{\text{Ser198}}-\text{N}_{\text{His438}})$  and  $R(\text{O}_{\text{Ser198}}-\text{C}_{\text{SuCh}})$  distances are 1.51 Å (1.56 Å for Asp70Gly) and 2.77 Å (2.64 Å for Asp70Gly), respectively, which should not hinder the nucleophilic attack of Ser198 and the concerted proton transfer from Ser198 to His438 in the first reaction step. In the enzyme–substrate complex, the strong hydrogen bond with a length of 1.76 Å (1.83 Å for Asp70Gly) is formed between the carboxyl oxygen atom of Glu 325 and the proton of His 438.

In the tetrahedral intermediate (Fig. 4), the distance between the oxygen atom of Ser 198 and the carbonyl carbon atom of molecule **2** is 1.44 Å (*cf.* 1.45 Å for Asp70Gly) and corresponds to the formation of a covalent bond. The ester group adopts a tetrahedral configuration. The  $\text{RC}-\text{C}(\text{O})-\text{OCH}_2\text{R}$  angle is  $\sim 120^\circ$ , which corre-

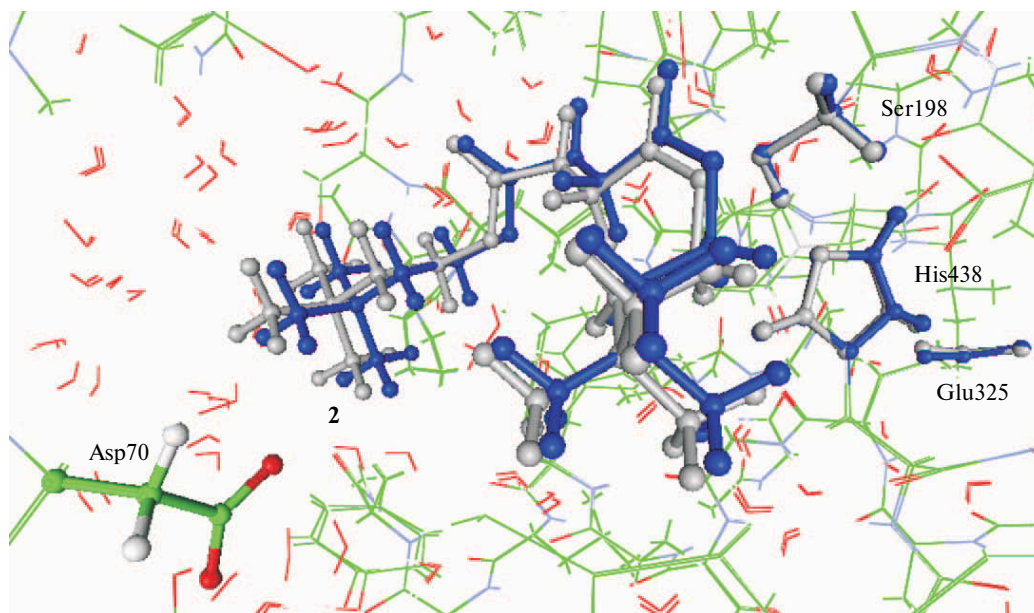
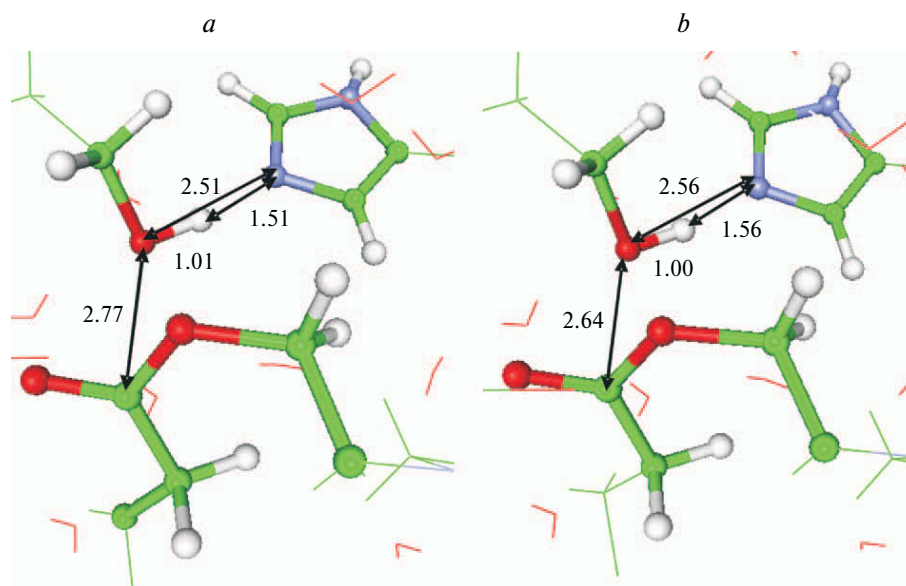


Fig. 2. Superimposition of the enzyme–substrate complexes for the unmodified (shown in pale) and modified enzymes (shown in dark).



**Fig. 3.** Geometry of the enzyme—substrate complex for the native (*a*) and modified (*b*) enzymes. The distances are given in Angströms.

sponds to the  $sp^3$  hybridization of the carbonyl carbon atom of the substrate. The  $N_{\text{His438}}^{\delta}-H_{\text{His438}}^{\delta}$  bond is slightly elongated (by 0.04 Å), and the proton is slightly shifted to the  $-\text{COO}^-$  group. In the modified enzyme, the distance between the oxygen atom of serine  $O_{\text{Ser198}}^{\gamma}$  and the nitrogen atom of histidine  $N_{\text{His438}}^{\epsilon}$  is 0.3 Å shorter than in the native enzyme, resulting in additional stabilization of the tetrahedral intermediate.

The geometry of the acyl-enzyme (Fig. 5) corresponds to the hydrolyzed substrate. The decomposition of the tetrahedral intermediate in the acylation step releases an alcohol (choline) molecule and the acyl-enzyme. The distance between  $O_{\text{Ser198}}^{\gamma}$  and  $C_{\text{SuCh}}$  is 1.31 Å (*cf.* 1.30 Å for Asp70Gly), which is indicative of the formation of a covalent bond between these atoms; the  $\text{RC}-\text{C}(\text{O})-\text{O}_{\text{Ser198}}$  angle is 175° (planar acyl group).

The total energies of the configurations corresponding to the stationary points on the PES of the system, which were obtained by the geometry optimization, were used to construct the energy profile of the reaction (Fig. 6).

It can be seen that the introduced mutation has no noticeable effect on the activation energy and, consequently, on the catalytic constant  $k_{\text{cat}}$ . This is evidence for an identical reaction mechanism. This result is consistent with the experimental data<sup>8</sup> showing that this mutation has the major effect on the Michaelis constant. Nevertheless, the effect of the introduced mutation on the total energy profile of the reaction manifests itself in stabiliza-

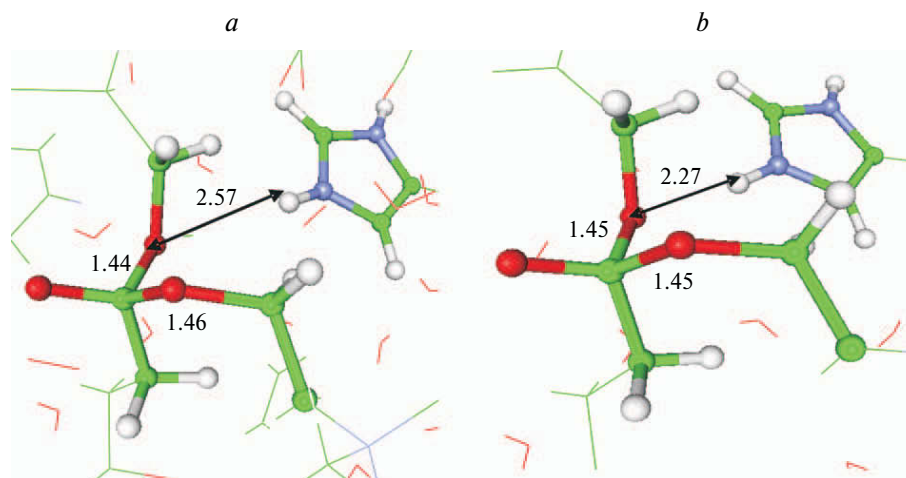


**Fig. 4.** Tetrahedral intermediate of the acylation step for the native (*a*) and modified (*b*) enzymes. The distances are given in Angströms.



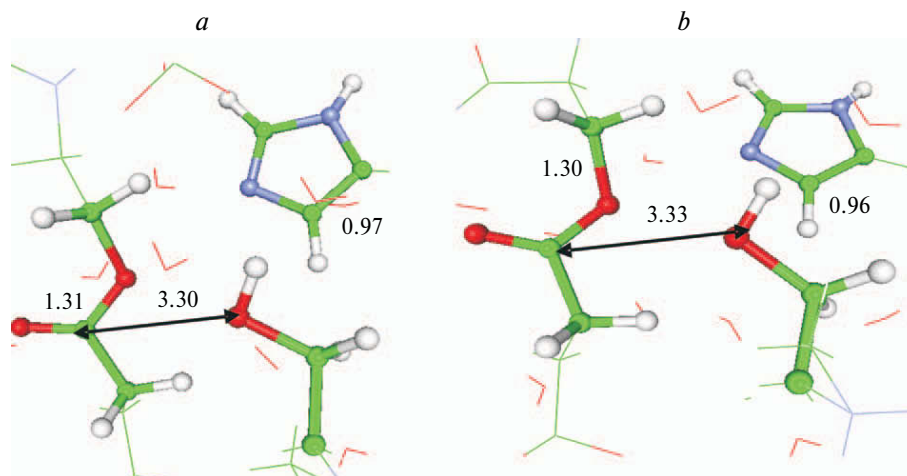


Fig. 5. Geometry of the acyl-enzyme for the native (*a*) and modified (*b*) enzymes. The distances are given in Angströms.

tion of the transition states. Electrostatic interactions between one of the choline fragments of the substrate and Asp70 cause a slight shift of the substrate away from the catalytic triad, whereas these interactions in the modified enzyme are absent, which leads to greater stabilization of the tetrahedral intermediate (see Figs 2 and 4) and to an increase in the energy gain from its formation by 3 kcal mol<sup>-1</sup>.

According to the tentative mechanism of hydrolysis, the initial acylation step involves the simultaneous nucleophilic attack of O<sup>γ</sup><sub>Ser198</sub> on the carbonyl carbon atom of the substrate and the transfer of the proton H<sup>γ</sup><sub>Ser198</sub> from serine to histidine to form the tetrahedral intermediate. By analyzing the changes in the geometry of the stationary points for the tetrahedral intermediate compared to the enzyme–substrate complex, the process can be monitored at the molecular level. As the *R*(O<sup>γ</sup><sub>Ser198</sub>–H<sup>γ</sup><sub>Ser198</sub>) distance decreases, resulting finally in the formation of

the covalent bond between these atoms, and the proton is transferred from Ser198 to His 438, the ester group is bent, adopts a tetrahedral configuration (sp<sup>3</sup> hybridization of the C<sub>SuCh</sub> atom), and becomes nonplanar (sp<sup>2</sup> hybridization of the C<sub>SuCh</sub> atom). The resulting tetrahedral intermediate is stabilized by hydrogen bonds between the negatively charged carbonyl oxygen atom O<sub>SuCh</sub> and the residues of the oxyanion hole.

The positively charged imidazolium cation that is formed upon the proton transfer from Ser198 to His438 is stabilized by electrostatic interactions with the closely spaced (~3.5 Å), negatively charged residues Glu325 and Glu197. An additional interaction with Glu197 leads to substantial stabilization of the tetrahedral intermediate lying 14 kcal mol<sup>-1</sup> (16 kcal mol<sup>-1</sup> for the Asp70Gly mutant) lower in energy than the enzyme–substrate complex.

The calculated barriers to the acylation step can be used to compare our results with the experimental data. The published<sup>26</sup> catalytic constant of hydrolysis of **2** is *k*<sub>cat</sub> = 500 s<sup>-1</sup>. In terms of the transition state theory, this gives the estimate of the energy barrier of about 14 kcal mol<sup>-1</sup>. Hence, the deacylation is the rate-limiting step.<sup>6</sup>

The transfer of the second proton between His438 and Glu325 in the acylation step (the possibility of this process was discussed in a series of studies<sup>14,27</sup>) does not occur. Our data showed that the protonation of His438 with the proton of Ser198 leads to only a slight elongation (by ~0.04 Å) of the N<sup>δ</sup><sub>His438</sub>–H<sup>δ</sup><sub>His438</sub> bond and an insignificant shift of the proton to Glu325 in the tetrahedral intermediate compared to the enzyme–substrate complex. Therefore, due to the stabilizing effect of Glu325 on the imidazolium cation, the one-proton mechanism is energetically more favorable. These results are in complete agreement with the results of our previous calculations of the hydrolysis in the active site of acetylcholinesterase, which is similar in the structure and the mechanism of hydrolysis to BuChE,<sup>13</sup> and also with other results of mod-

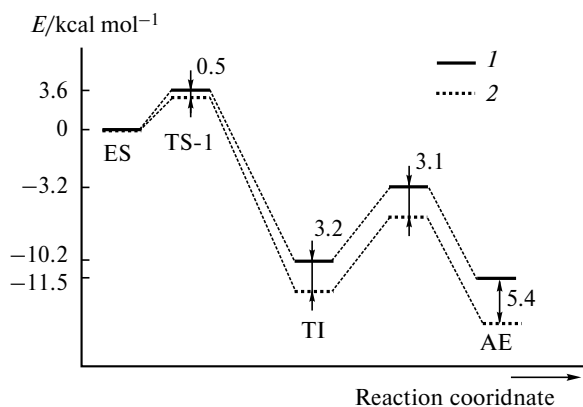


Fig. 6. Calculated energy barriers (kcal mol<sup>-1</sup>) for the acylation step of hydrolysis of **2** by the native BuChE (*1*) and modified BuChE (*2*) with the single mutation Asp70Gly. ES is the enzyme–substrate complex, TI is the tetrahedral intermediate, and AE is the acyl-enzyme.

eling of the mechanisms of hydrolysis of serine proteases<sup>28</sup> and carboxypeptidases.<sup>10</sup>

To sum up, the results of QM/MM simulation showed that the Asp70Gly single mutation of butyrylcholinesterase does not lead to the qualitatively different energy profile of the hydrolysis of succinylcholine for the acylation step compared to the native enzyme. The quantitative differences in the activation barriers are also small. However, the modified enzyme is characterized by greater stabilization of the tetrahedral intermediate.

We thank the Joint Supercomputer Center of the Russian Academy of Sciences for providing the computing time on an MVS-100K supercomputer (<http://www.jscc.ru>), the Belarusian—Russian Union State (SKIF-GRID research-technical program), the Interregional Computer Center of the Tomsk State University for providing the computing time on a SKIF-Cyberia supercomputer, and the Scientific-Research Computer Center of the M. V. Lomonosov for providing the computing time on a SKIF-MGU supercomputer.

The present study was in part financially supported by the Russian Foundation for Basic Research (Project No. 10-03-00085) and the Russian Academy of Sciences (Program 9 of the Division of Chemistry and Materials Science of the Russian Academy of Sciences).

## References

1. M. Barbosa, O. Rios, M. Velásquez, J. Villalobos, J. Ehrmanns, *Surg. Neurol.*, 2001, **55**, 106.
2. C.-G. Zhan, F. Zheng, D. W. Landry, *J. Am. Chem. Soc.*, 2003, **125**, 2462.
3. L. G. Sokolovskaya, L. V. Sigolaeva, A. V. Eremenko, I. N. Kurochkin, G. F. Makhaeva, V. V. Malygin, I. E. Zykova, V. I. Kholstov, N. V. Zav'yalova, S. D. Varfolomeev, *Khim. Biol. Bezopasnost' [Chem. Biol. Safety]*, 2004, **13**—**14**, 21 (in Russian).
4. M. Pirmohamed, B. K. Park, *Trends Pharmacol. Sci.*, 2001, **22**, 298.
5. M. C. McGuire, C. P. Nogueira, C. F. Bartels, H. Lightstone, A. Hajra, A. F. Van der Spek, O. Lockridge, B. N. La Du, *Proc. Natl. Acad. Sci. USA*, 1989, **86**, 953.
6. D. Suarez, N. Diaz, J. Fontecilla-Camps, M. J. Field, *Biochemistry*, 2006, **45**, 7529.
7. C.-G. Zhan, D. Gao, *Biophys. J.*, 2005, **89**, 3863.
8. P. Masson, P. Legrand, C. F. Bartels, M.-T. Froment, L. M. Schopfer, O. Lockridge, *Biochemistry*, 1997, **36**, 2266.
9. S. D. Varfolomeev, *Khimicheskaya enzimologiya [Chemical Enzymology]*, Akademiya, Moscow, 2005, 480 pp. (in Russian).
10. K. B. Bravaya, A. V. Bochenkova, B. L. Grigorenko, I. A. Topol, S. Burt, A. V. Nemukhin, *J. Chem. Theory Comput.*, 2006, **2**, 1168.
11. B. L. Grigorenko, A. V. Nemukhin, M. S. Shadrina, I. A. Topol, S. K. Burt, *Proteins: Structure, Function, Bioinformatics*, 2007, **66**, 456.
12. B. L. Grigorenko, A. V. Rogov, I. A. Topol, S. K. Burt, H. M. Martinez, A. V. Nemukhin, *Proc. Natl. Acad. Sci.*, 2007, **104**, 7057.
13. A. V. Nemukhin, S. V. Lushchekina, A. V. Bochenkova, A. A. Golubeva, S. D. Varfolomeev, *J. Mol. Model.*, 2008, **14**, 409.
14. Y. Zhang, J. Kua, J. A. McCammon, *J. Am. Chem. Soc.*, 2002, **124**, 10572.
15. H. M. Berman, J. Westbrook, Z. Feng, G. Gilliland, T. N. Bhat, H. Weissig, I. N. Shindyalov, P. E. Bourne, *Nucleic Acids Res.*, 2000, **28**, 235.
16. J. M. Word, S. C. Lovell, T. H. Labean, H. C. Taylor, M. E. Zalis, B.K. Presley, J. S. Richardson, D. C. Richardson, *J. Mol. Biol.*, 1999, **285**, 1711.
17. D. M. Quinn, *Chem. Rev.*, 1987, **87**, 955.
18. M. A. Massiah, C. Viragh, P. M. Reddy, I. M. Kovach, J. Johnson, T. L. Rosenberry, A. S. Mildvan, *Biochemistry*, 2001, **40**, 5682.
19. G. M. Morris, D. S. Goodsell, R. S. Halliday, R. Huey, W. E. Hart, R. K. Belew, A. J. Olson, *J. Am. Chem. Soc.*, 1998, **120**, 1639.
20. J. W. Ponder, *TINKER: Software Tools for Molecular Design*, Version 3.7, 1999, Washington University: St. Louis.
21. T. A. Halgren, *J. Comput. Chem.*, 1996, **17**, 490.
22. B. L. Grigorenko, A. V. Nemukhin, I. A. Topol, S. K. Burt, *J. Phys. Chem. A*, 2002, **106**, 10663.
23. A. V. Nemukhin, B. L. Grigorenko, I. A. Topol, S. K. Burt, *J. Comput. Chem.*, 2003, **24**, 1410.
24. J. Wang, R. M. Wolf, J. W. Caldwell, P. A. Kollman, D. A. Case, *J. Comput. Chem.*, 2004, **25**, 1157.
25. A. A. Granovsky, *PC GAMESS/Firefly version 7.1.F*, <http://classic.chem.msu.su/gran/gamess/index.html>.
26. P. Masson, M.-T. Froment, P. L. Fortier, J. E. Visicchio, C. F. Bartels, O. Lockridge, *Biochim. Biophys. Acta Prot. Struct. Mol. Enzym.*, 1998, **1387**, 41.
27. M. Fuxreiter, A. Warshel, *J. Am. Chem. Soc.*, 1998, **120**, 183.
28. A. V. Nemukhin, B. L. Grigorenko, A. V. Rogov, I. A. Topol, S. K. Burt, *Theor. Chem. Acc.*, 2004, **111**, 36.

Received July 8, 2009;  
in revised form October 14, 2009